

## Geometric Dependence of ${}^3\text{h}J({}^{31}\text{P}-{}^{15}\text{N})$ and ${}^2\text{h}J({}^{31}\text{P}-{}^1\text{H})$ Scalar Couplings in Protein–Nucleotide Complexes

Jiri Czernek<sup>†</sup> and Rafael Brüschweiler\*

Gustaf H. Carlson School of Chemistry and Biochemistry  
Clark University, Worcester, Massachusetts 01610

Received July 3, 2001

Since their first observation in 1998,<sup>1</sup> indirect electron-mediated interactions between nuclear spins across hydrogen bonds in biomolecules have become an important tool for the structural characterization of biological macromolecules (see reference 2 for a review). These couplings have also become the focus of quantum-chemical investigations.<sup>3–7</sup> Recently, experimental three-bond  ${}^3\text{h}J({}^{31}\text{P}-{}^{15}\text{N})$  ( ${}^3\text{h}J_{\text{PN}}$ ) and two-bond  ${}^2\text{h}J({}^{31}\text{P}-{}^1\text{H})$  ( ${}^2\text{h}J_{\text{PH}}$ ) scalar couplings across N–H···O–P hydrogen bonds of protein–nucleotide complexes were reported by Mishima et al.<sup>8</sup> and by Löhrl et al.<sup>9</sup> In the former work, a strong dependence of these couplings on the hydrogen-bond geometry in the complex between GDP nucleotide and Ras p21 protein was found.<sup>8</sup>

We present calculations of  ${}^3\text{h}J_{\text{PN}}$  and  ${}^2\text{h}J_{\text{PH}}$  couplings for this protein–nucleotide complex using the DFT-based methodology of Malkin et al.,<sup>10</sup> which is well-suited to study spin–spin couplings in sizable systems,<sup>11,12</sup> and compare the results with experimentally determined  $J$  couplings by Mishima et al.<sup>8</sup> An analytical parametrization of calculated couplings is derived that reflects their distinct dependence on the hydrogen-bonding geometry and which facilitates the structural interpretation of these new types of NMR parameters.

DFT calculations were applied to coordinate sets of model compounds, which were generated as follows. Coordinates of amino acid residues Gly13, Gly15, Lys16, and Ser17 of Ras p21 (including side-chain atoms) that form hydrogen bonds with the phosphorus of GDP were extracted from the 2.2 Å resolution

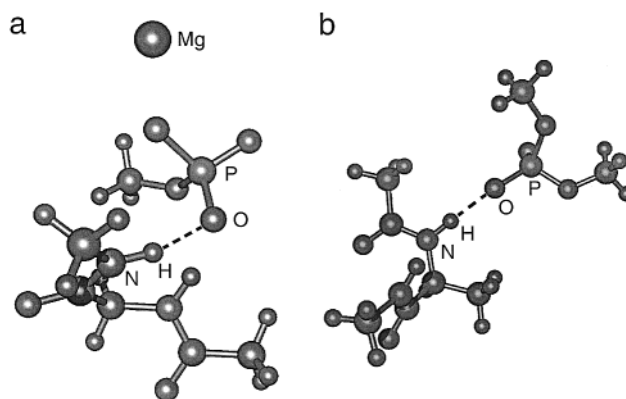


**Figure 1.** (a) Model of Gly15 together with  $\text{Mg}[\text{PO}_4(\text{CH}_3)]$  as used for calculations of  ${}^3\text{h}J_{\text{PN}}$  and  ${}^2\text{h}J_{\text{PH}}$  couplings in the residues Gly13, Gly15, Lys16, and Ser17. The P–O–H arrangement, which departs from linearity, in the N–H···O–P fragment is shown. (b) Model of Ala18 together with  $[\text{PO}_4(\text{CH}_3)_2]^-$  as used for DFT calculations of geometrical dependence of  ${}^3\text{h}J_{\text{PN}}$  and  ${}^2\text{h}J_{\text{PH}}$  couplings in GDP–Ras p21 complex. The nearly linear P–O–H arrangement in the N–H···O–P fragment is shown.

X-ray structure (PDB entry 1Q21).<sup>13</sup> Coordinates were also extracted for Ala18, which is hydrogen-bonded to the phosphorus of GDP.<sup>13,14</sup> Each residue was truncated at its N terminus with an acetyl group and at its C terminus with a *N*-methylamino group with atoms placed at the positions of atoms of the neighboring residues in the crystal structure.<sup>13</sup> To speed up calculations, simplified models for the phosphorus-containing fragments of GDP were used. The  $\alpha$ -phosphorus of GDP and its covalently bonded neighbor atoms were modeled as magnesium methyl phosphate ( $\text{Mg}[\text{PO}_4(\text{CH}_3)]$ , see Figure 1a), while the  $\beta$ -phosphorus of GDP and its environment were represented as dimethyl ester of phosphoric acid anion ( $[\text{PO}_4(\text{CH}_3)_2]^-$ , Figure 1b).

Calculations of trans-hydrogen bond scalar  $J$ -coupling constants were performed, including the Fermi-contact (FC) term, paramagnetic spin–orbit (PSO) term, the diamagnetic spin–orbit (DSO) term using the deMon-NMR code<sup>10,15,16</sup> adopting the procedure that was successfully applied to biomolecular systems.<sup>5,7</sup> The Perdew and Wang<sup>17</sup> semilocal exchange functional and the correlation functional of Perdew<sup>18</sup> were employed. The PSO term was calculated with the Loc.1 approximation of SOS-DFPT<sup>19</sup> using a grid consisting of 32 points of radial quadrature. In the FC calculations, a grid with 64 radial points and the perturbation of 0.001 at the position of phosphorus nucleus were applied. The IGLO-III basis set<sup>20</sup> was used, except for magnesium which was treated with the small effective-core potential valence basis of ref 21.

NMR measurements of the GDP complexes of the wild-type Ras protein and the human Ras p21 Q61L-substituted protein yield

\* To whom correspondence should be addressed. Professor Rafael Brüschweiler, Carlson School of Chemistry and Biochemistry, Clark University, Worcester, MA 01610-1477. Telephone: (508) 793-7220. Fax: (508) 793-8861. E-Mail: bruschiweil@nmr.clarku.edu.

<sup>†</sup> On leave from Institute of Macromolecular Chemistry, Academy of Sciences of the Czech Republic, Heyrovsky Sq. 2, 162 06 Praha 6, Czech Republic.

(1) Dingley, A. J.; Grzesiek, S. *J. Am. Chem. Soc.* **1998**, *120*, 8293–8297.  
(2) Zidek, L.; Stefl, R.; Sklenar, V. *Curr. Opin. Struct. Biol.* **2001**, *11*, 275–281.

(3) Dingley, A. J.; Masse, J. E.; Peterson, R. D.; Barfield, M.; Feigon, J.; Grzesiek, S. *J. Am. Chem. Soc.* **1999**, *121*, 6019–6027.

(4) Barfield, M.; Dingley, A. J.; Feigon, J.; Grzesiek, S. *J. Am. Chem. Soc.* **2001**, *123*, 4014–4022.

(5) Scheurer, C.; Brüschweiler, R. *J. Am. Chem. Soc.* **1999**, *121*, 8661–8862.

(6) Shenderovich, I. G.; Smirnov, S. N.; Denisov, G. S.; Gindin, V. A.; Golubev, N. S.; Dunger, A.; Reibke, R.; Kirpekar, S.; Malkina, O. L.; Limbach, H.-H. *Ber. Bunsen-Ges. Phys. Chem.* **1998**, *102*, 422–428. Benedict, H.; Shenderovich, I. G.; Malkina, O. L.; Malkin, V. G.; Denisov, G. S.; Golubev, N. S.; Limbach, H.-H. *J. Am. Chem. Soc.* **2000**, *122*, 1979–1988. Del Bene, J. E.; Perera, S. A.; Bartlett, R. J. *J. Am. Chem. Soc.* **2000**, *122*, 3560–3561. Del Bene, J. E.; Bartlett, R. J. *J. Am. Chem. Soc.* **2000**, *122*, 10480–10481. Pecul, M.; Leszczynski, J.; Sadlej, J. *J. Phys. Chem. A* **2000**, *104*, 8105–8113. Galasso, V. *Int. J. Quantum Chem.* **1998**, *70*, 313–320. Bagno, A. *Chem.–Eur. J.* **2000**, *6*, 2925–2930.

(7) Arnold, W. D.; Mao, J.; Sun, H.; Oldfield, E. *J. Am. Chem. Soc.* **2000**, *122*, 12164–12168.

(8) Mishima, M.; Hatanaka, M.; Yokohama, S.; Ikegami, T.; Walchli, M.; Ito, Y.; Shirakawa, J. *J. Am. Chem. Soc.* **2000**, *122*, 5883–5884.

(9) Löhrl, F.; Mayhew, S. G.; Rüterjans, H. *J. Am. Chem. Soc.* **2000**, *122*, 9289–9295.

(10) Malkin, V. G.; Malkina, O. L.; Salahub, D. R. *Chem. Phys. Lett.* **1994**, *221*, 91–99.

(11) Czernek, J.; Lang, J.; Sklenar, V. *J. Phys. Chem. A* **2000**, *104*, 2788–2792.

(12) Case, D. A.; Scheurer, C.; Brüschweiler, R. *J. Am. Chem. Soc.* **2000**, *122*, 10390–10397.

(13) Tong, L. A.; de Vos, A. M.; Milburn, M. V.; Kim, S. H. *J. Mol. Biol.* **1991**, *217*, 503–516.

(14) Kraulis, P. J.; Domaille, P. J.; Campbell-Burk, S. L.; Van Aken, T.; Laue, E. D. *Biochemistry* **1994**, *33*, 3515–3531.

(15) Malkin, V. G.; Malkina, O. L.; Eriksson L. A.; Salahub, D. R. In *Modern Density Functional Theory: A Tool for Chemistry*; Seminario, J. M., Politzer, P., Eds.; Elsevier: Amsterdam, 1995; Vol. 2, p 273.

(16) Salahub, D. R.; Fournier, R.; Mlynarski, P.; Papai, A.; St-Amant, A.; Uskio, J. In *Density Functional Methods in Chemistry*; Labanowski, J., Andzelm, J. W., Eds.; Springer: New York, 1991; p 77.

(17) Perdew, J. P.; Wang, Y. *Phys. Rev. B* **1986**, *33*, 8800–8810.

(18) Perdew, J. P. *Phys. Rev. B* **1986**, *33*, 8822–8825; **1986**, *34*, 7406.

(19) Malkin, V. G.; Malkina, O. L.; Casida, M. E.; Salahub, D. R. *J. Am. Chem. Soc.* **1994**, *116*, 5898–5908.

(20) Kutzelnigg, W.; Fleischer, U.; Schindler, M. In *NMR: Basic Principles and Progress*; Springer-Verlag: Heidelberg, 1990; Vol. 23, p 165.

(21) Kaupp, M.; Stoll, H.; Preuss, H. *J. Comput. Chem.* **1990**, *11*, 1029–1037.

**Table 1:** Hydrogen Bond Lengths and Angles of Ras p21–Nucleotide Complex Together with  $^3J_{\text{PN}}$  and  $^2J_{\text{PH}}$  Coupling Values

residue	$r_{\text{NO}}$ [Å]	$\alpha_{\text{POH}}$ [deg]	$\alpha_{\text{OHN}}$ [deg]	$^3J_{\text{PN}}$ [Hz] <sup>a,b</sup>	$^2J_{\text{PH}}$ [Hz] <sup>a,b</sup>
Gly13	2.76	108	171	−0.24 (<0.27)	−0.90 (<0.52)
Gly15	2.74	110	162	−0.07 (<0.53)	−0.88 (<0.92)
Lys16	2.77	116	165	+0.37 (<0.35)	−0.38 (<0.98)
Ser17	3.05	119	157	+0.31 (<0.29)	+0.18 (<0.26)
Ala18	2.85	175	149	−4.00 (4.62 ± 0.01)	−3.26 (3.36 ± 0.09)

<sup>a</sup> Calculated couplings together with experimental couplings in parentheses. <sup>b</sup> Signs of experimental  $^3J_{\text{PN}}$  and  $^2J_{\text{PH}}$  data have not been determined.

rather weak spin–spin couplings (below 1 Hz) between acceptor groups of GDP and amidic ( $^1\text{H}$  and  $^{15}\text{N}$ ) nuclei of Gly13, Gly15, Lys16, and Ser17.<sup>8</sup> This is confirmed by our DFT calculations of the corresponding model structures where computed  $^3J_{\text{PN}}$  and  $^2J_{\text{PH}}$  couplings do not exceed 0.37 Hz and −0.90 Hz, respectively. The situation differs for Ala18 for which sizable  $^3J_{\text{PN}}$  and  $^2J_{\text{PH}}$  couplings of 4.62 and 3.36 Hz were measured. They are nearly quantitatively reproduced by the calculations (Table 1). It should be noted that both Ala18 couplings are computed to be negative, while experimentally the sign of the two couplings was found to be the same, but the absolute sign could not be determined.<sup>8</sup>

There are distinct differences in the contributions of FC, PSO, and DSO terms to the  $^3J_{\text{PN}}$  and  $^2J_{\text{PH}}$  couplings in Ala18. The PSO and DSO terms both have positive signs whereas the FC terms is always negative.  $^3J_{\text{PN}}$  couplings are dominated by the FC term: for all structures investigated, the sum of PSO and DSO contributions amounts to less than 3% of the FC value. In contrast, PSO and DSO terms contribute on average about one-third of the total  $^2J_{\text{PH}}$  value. In the case of Ala18 the FC, PSO, and DSO terms are −4.54 Hz, +1.03 Hz, and +0.25 Hz, respectively, which illustrates the importance of noncontact terms for the accurate prediction of this coupling (experimental value in the Ras(Q61L)–GDP complex is (−) 3.36 ± 0.09 Hz.<sup>8</sup>).

Mishima et al.<sup>8</sup> et al. noticed that the large variation in the  $^3J_{\text{PN}}$  and  $^2J_{\text{PH}}$  couplings between Ala18 and Gly13, Gly15, Lys16, and Ser17 does not correlate with changes in hydrogen-bond lengths: according to the crystal structure<sup>13</sup> the NO distance for Ala18 is shorter than for Ser17 but longer than for Gly13, Gly15, and Lys16 (Table 1). As judged from backbone  $^{15}\text{N}$  relaxation measurements, this difference also cannot be attributed to effects of fast dynamics.<sup>14,22</sup> Their conclusion<sup>8</sup> that the approximately linear hydrogen-bonding arrangement as expressed by the POH angle (and not by the OHN angle, which remains fairly constant for all five residues, see Table 1) is a prerequisite for the presence of large  $^3J_{\text{PN}}$  and  $^2J_{\text{PH}}$  couplings is fully supported by the present calculations. A dramatic increase in  $^3J_{\text{PN}}$  and  $^2J_{\text{PH}}$  values is observed by setting the POH angle to 175° in the complexes involving Gly13 and Gly15 (which is the value of this angle for Ala18 in the X-ray structure), while keeping the NO distance fixed at 2.76 and 2.74 Å, respectively (see Table S1).

Two-dimensional surfaces of the  $^3J_{\text{PN}}$  and  $^2J_{\text{PH}}$  couplings were calculated for the Ala18 model as a function of the NO distance and the POH angle (Figure 2) and parametrized by an expression that factorizes radial and angular parts:

$$^{\text{nh}}J_{\text{PX}}(r_{\text{NO}}, \alpha_{\text{POH}}) = a_0 e^{-a_1 r_{\text{NO}}} \{\cos(\alpha_{\text{POH}} - \alpha_{\text{offset}})\}^{a_2} \quad (1)$$

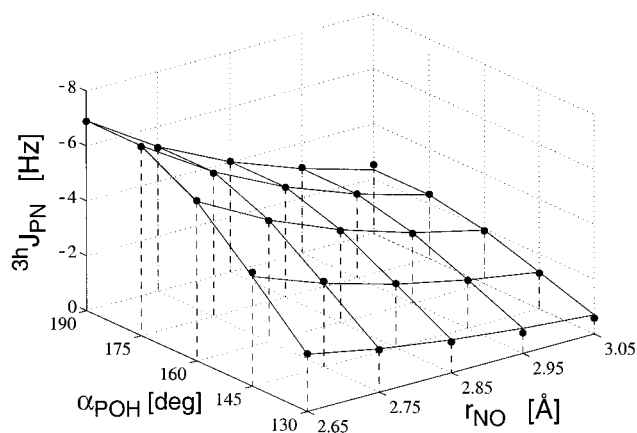


**Figure 2.**  $^3J_{\text{PN}}$  couplings in the model of Ala18 as a function of the  $r_{\text{NO}}$  distance and the  $\alpha_{\text{POH}}$  angle. The surface shows the data fitted to the DFT values (using eq 1) represented as stems. An analogous figure for the  $^2J_{\text{PH}}$  coupling together with Tables of calculated couplings are given in the Supporting Information.

For the  $^3J_{\text{PN}}$  couplings ( $n = 3$ ,  $X = \text{N}$ ) the optimal parameters are  $a_0 = -9628.6$  Hz,  $a_1 = 2.7232 \text{ \AA}^{-1}$ ,  $a_2 = 2.4761$ ,  $\alpha_{\text{offset}} = 3.1853$  rad, while for the  $^2J_{\text{PH}}$  couplings ( $n = 2$ ,  $X = \text{H}$ ) they are  $a_0 = -28446$  Hz,  $a_1 = 3.1969 \text{ \AA}^{-1}$ ,  $a_2 = 1.9133$ ,  $\alpha_{\text{offset}} = 3.1068$  rad. For the 25 computed  $^3J_{\text{PN}}$  and  $^2J_{\text{PH}}$  couplings the sum of squared differences between DFT and eq 1 is  $\chi^2 = 0.125$  Hz<sup>2</sup> and  $\chi^2 = 0.476$  Hz<sup>2</sup>, respectively, with maximum deviation of only 0.18 and 0.19 Hz, respectively.

The  $^3J_{\text{PN}}$  and  $^2J_{\text{PH}}$  couplings sensitively probe the hydrogen-bond angle and distance in a way that is well captured by eq 1. They exponentially decrease with increasing NO distance, which is consistent with previous experimental<sup>23</sup> and theoretical<sup>5,24</sup> findings for  $^3J_{\text{NC}}$  trans-hydrogen bond couplings in proteins and  $^2J_{\text{NN}}$  couplings in nucleic acids.<sup>3,4</sup> The combined application of the parametrizations of eq 1 to experimental  $^3J_{\text{PN}}$  and  $^2J_{\text{PH}}$  couplings, in a way analogous to the widely used Karplus-type relationships, provides useful constraints for the determination of the structures of protein–nucleotide complexes in solution.

**Acknowledgment.** We thank Drs. J.-C. Hus and J. J. Prompers for technical assistance. The initial stage of this project has been sponsored by the Grant Agency of the Academy of Sciences of the Czech Republic through the Grant 14/96K (reg. c. K2055603). Time allocation in the Czech Academic Supercomputer Centre is gratefully acknowledged. This work was supported by NSF Grant MCB-9904875.

**Supporting Information Available:** Three tables and one figure containing calculated  $^3J_{\text{PN}}$  and  $^2J_{\text{PH}}$  couplings between phosphate and glycines (Table S1) and Ala18 (Tables S2 and S3, Figure S4) for different bonding arrangements (PDF). This material is available free of charge via the Internet at <http://pubs.acs.org>.

JA011618R

(22) Ito, Y.; Yamasaki, K.; Iwahara, J.; Terada, T.; Kamiya, A.; Shirouzu, M.; Muto, Y.; Kawai, G.; Yokohama, S.; Laue, E. D.; Walchli, M.; Shibata, T.; Nishimura, S.; Miyazawa, T. *Biochemistry* **1997**, *36*, 9109–9119.

(23) Cornilescu, G.; Hu, J.-S.; Bax, A. *J. Am. Chem. Soc.* **1999**, *121*, 2949–2950.

(24) Arnold, W. D.; Oldfield, E. *J. Am. Chem. Soc.* **2000**, *122*, 12835–12841.